

Journal of Mechanics of Materials and Structures

STUDY OF MULTIPLY-LAYERED CYLINDERS MADE OF FUNCTIONALLY
GRADED MATERIALS USING THE TRANSFER MATRIX METHOD

Y. Z. Chen

Volume 6, No. 5

May 2011

STUDY OF MULTIPLY-LAYERED CYLINDERS MADE OF FUNCTIONALLY GRADED MATERIALS USING THE TRANSFER MATRIX METHOD

Y. Z. CHEN

This paper provides a general solution for a multiply-layered cylinder made of functionally graded materials. The Young's modulus is assumed to be an arbitrary function of r , and the Poisson's ratio takes a constant value. The first step is to study the single-layer case ($a < r < b$). A transfer matrix is defined, relating the values of radial stress and displacement at the initial point ($r = a$) to those at the end point ($r = b$). The matrix is evaluated on the basis of two fundamental solutions, which are evaluated numerically. The final solution is obtained by using many transfer matrices for layers, continuation conditions between layers, and boundary conditions at inner and outer boundaries. Several numerical examples are provided.

1. Introduction

Functionally graded materials (FGMs) are widely used in industries such as space structures and fusion reactors. Therefore, elastic analysis of structures made of FGMs has attracted many researchers. FGMs are nonhomogeneous elastic mediums. The elastic properties of FGMs are variable with the respect to spatial location. The difficulties of solving elastic FGM problems can be easily seen. Taking the plane elasticity problem of FGMs as an example, the complex variable method is no longer useful in this case. Therefore, it is necessary to develop appropriate methods to solve some problems for FGMs.

Clearly, it is difficult to study the three-dimensional elasticity of FGMs. Researchers have paid attention to some particular problems for FGMs. For example, crack problems for an elastic medium made of FGMs were investigated in [Erdogan and Wu 1997; Jain et al. 2004; Fotuhi and Fariborz 2006].

One topic to investigate regarding FGMs is the stress distribution in a thick cylinder of FGMs. The elasticity problem of a homogeneous hollow circular cylinder has been solved by [Muskhelishvili 1963; Timoshenko and Goodier 1970].

Earlier research for thick cylinder FGMs was proposed [Horgan and Chan 1999a; 1999b]. A solution for the pressurized hollow cylinder or disk problem for functionally graded isotropic linearly elastic materials was achieved. The material and the thermal properties were assumed to vary along the radius r according to a power law function.

Recently, many research works have been devoted to the hollow circular cylinder problem for FGMs [Zhang and Hasebe 1999; Shao 2005; Dryden and Jayaraman 2006; Shi et al. 2007; Tutuncu 2007; Batra and Iaccarino 2008; Chen and Lin 2008; Theotokoglou and Stampoulglou 2008; Li and Peng 2009]. In most of the studies, the Young's modulus is assumed in the form of exponential or power law functions. Thus, the suggested techniques are no longer useful for an arbitrary Young's modulus distribution. In the case of a Young's modulus expression $E(r) = E_0(r/a)^n$, a closed form solution

Keywords: composites, layered structure, nonlinear behavior, transfer matrix method, strength.

for displacement was obtained [Horgan and Chan 1999a; 1999b]. In the case of a Young's modulus expression $E(r) = E_0 \exp \beta r$, an ordinary differential equation for displacement was suggested [Tutuncu 2007]. To obtain the final solution, one needs to complete a detailed derivation.

If the Young's modulus is an arbitrary function, one needs to derive a numerical method to solve the problem. For example, the associated elastic problem is reduced to a Fredholm integral equation. By approximately solving the resulting equation, the distributions of the radial and circumferential stresses can be determined [Li and Peng 2009].

Some papers were devoted to a multiply-layered cylinder [Zhang and Hasebe 1999; Shi et al. 2007]. However, the homogeneous condition was assumed for individual layers. This means that a cylinder of FGMs is approximated by many homogeneous layers, and the nonhomogeneous condition is not considered in individual layers.

In addition, some papers were devoted to the hollow sphere problem for FGMs [Eslami et al. 2005; You et al. 2005; Chen and Lin 2008]. The solution technique is approximately same as in the case of a hollow cylinder.

Axisymmetric displacements and stresses in functionally-graded hollow cylinders, disks, and spheres subjected to uniform internal pressure were determined using plane elasticity theory and the complementary functions method [Tutuncu and Temel 2009].

This paper provides a general solution for a multiply-layered cylinder of FGMs. The Young's modulus is assumed to be an arbitrary function with respect to r , and the Poisson's ratio takes a constant value. The first step is to study the single-layer case. A transfer matrix \mathbf{M} is defined for the single-layer case ($a < r < b$). The matrix relates the values of radial stress and displacement at the initial point ($r = a$) to those at the end point ($r = b$). The matrix is evaluated on the basis of two fundamental solutions, which are evaluated numerically. By using many transfer matrices for layers, continuation conditions between layers, and boundary conditions at inner and outer boundaries, the final solution is obtained.

The suggested formulation can be used in the case of an arbitrary Young's modulus. In this paper, the Young's modulus is assumed in the form of an exponential function with respect to r , and Poisson's ratio takes a constant value. Numerical examples for a three-layered cylinder are carried out. It is found that the factor β in the expression of the Young's modulus has significant influence on the distribution of stresses.

2. Boundary value problem for a single-layer cylinder

Since the solution for a multiply-layered cylinder has a close relation to the case of a single-layer cylinder, a formulation for the boundary value problem for a single-layer cylinder is introduced below.

2.1. Elastic analysis for a thick cylinder made of FGM. A long cylinder with inner radius a and outer radius b is investigated (Figure 1). The cylinder is assumed under some traction or displacement boundary value conditions at the inner boundary ($r = a$) and outer boundary ($r = b$).

The problem can be studied in polar coordinates (r, θ) . In the symmetrical deformation case, the displacement in the r -direction is denoted by u . Two strain components can be expressed as follows (see [Muskhelishvili 1963; Timoshenko and Goodier 1970]):

$$\varepsilon_r = \frac{du}{dr}, \quad \varepsilon_\theta = \frac{u}{r} \quad (u = \varepsilon_\theta r). \quad (1)$$

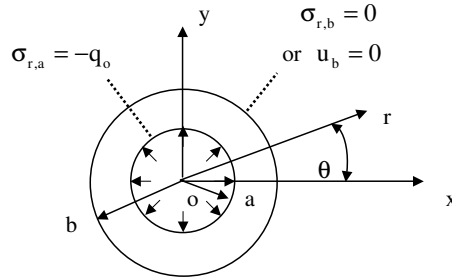


Figure 1. Two typical boundary conditions: (a) $\sigma_{r,a} = -q_0$ at $r = a$, $\sigma_{r,b} = 0$ at $r = b$ and (b) $\sigma_{r,a} = -q_0$ at $r = a$, $u_b = 0$ at $r = b$.

From (1), the compatibility condition of displacement will be

$$\varepsilon_r = \frac{d(r\varepsilon_\theta)}{dr}, \quad \text{or} \quad \varepsilon_r = \varepsilon_\theta + r \frac{d\varepsilon_\theta}{dr}. \tag{2}$$

For the stress components σ_r and σ_θ , the equilibrium equation takes the form

$$\frac{d\sigma_r}{dr} + \frac{\sigma_r - \sigma_\theta}{r} = 0. \tag{3}$$

Equation (3) can be satisfied automatically, if one introduces a function $F(r)$ and lets

$$\sigma_r = \frac{F(r)}{r}, \quad \sigma_\theta = \frac{dF}{dr}. \tag{4}$$

The following derivation is suitable not only for the continuous case of the Young’s modulus $E(r)$ and the Poisson’s ratio $\nu(r)$ but also for the discontinuous case of $E(r)$ and $\nu(r)$. Therefore, the suggested approach can be used in the general case.

In this paper, it is assumed that the Poisson’s ratio ν ($= 0.3$) takes a constant value. In addition, one type of the Young’s modulus takes the following form:

$$E(r) = E_0 \exp[\beta(r - a)/(b - a)], \quad \text{with} \quad E(r)|_{r=a} = E_0, \quad E(r)|_{r=b} = E_0 \exp \beta \quad (a \leq r \leq b), \tag{5}$$

where E_0 is a constant, and β takes a negative or positive value and represents the property of the FGMs, hereafter called the material parameter. It will be seen later that the suggested technique is valid for an arbitrary function $E(r)$.

In the formulation, the material properties of the FGM are continuous functions of position. Generally, the material coefficients of FGM manufactured in a perfect process are changed in space without acuity. From (5), we can define a ratio by $\gamma = E(r)|_{r=b}/E(r)|_{r=a}$ or $\gamma = \exp(\beta)$. The value γ represents the ratio of the Young’s modulus at the outer boundary and at the inner boundary. If $\beta = 0$, $\beta = 0.1$, $\beta = 0.2$, and $\beta = 1$, we have $\gamma = 1$, $\gamma = 1.1052$, $\gamma = 1.2214$, and $\gamma = 2.7183$, respectively. Therefore, (5) can model the material properties of FGM when the properties are not changed significantly along the radial direction.

In the plane strain case, the stress-strain relation will be

$$\varepsilon_r = \frac{1 - \nu^2}{E(r)} \left(\sigma_r - \frac{\nu}{1 - \nu} \sigma_\theta \right), \quad \varepsilon_\theta = \frac{1 - \nu^2}{E(r)} \left(\sigma_\theta - \frac{\nu}{1 - \nu} \sigma_r \right), \tag{6}$$

where the Young's modulus $E(r)$ is an arbitrary function. From (1), (4), and (6), the displacement component u can be expressed as

$$u = \varepsilon_{\theta} r = \frac{(1 - \nu^2)r}{E(r)} \left(\frac{dF}{dr} - \frac{\nu}{1 - \nu} \frac{F}{r} \right). \quad (7)$$

Substituting (4) into (6) and then (6) into (2) yields

$$\frac{d^2 F}{dr^2} + \frac{1}{r} \frac{dF}{dr} - \frac{F}{r^2} - \left(\frac{dF}{dr} - \frac{\nu}{1 - \nu} \frac{F}{r} \right) p(r) = 0, \quad \text{where } p(r) = \frac{1}{E(r)} \frac{dE(r)}{dr} \quad (\text{or } \Lambda(F(r)) = 0). \quad (8)$$

If the function $E(r)$ is given by (5), we have

$$p(r) = \frac{\beta}{b - a}. \quad (9)$$

Alternatively, if $E(r)$ is defined by

$$E(r) = E_0 [1 + (\exp \beta - 1)(r - a)/(r - b)], \quad E(r)|_{r=a} = E_0, \quad E(r)|_{r=b} = E_0 \exp \beta \quad (a \leq r \leq b), \quad (10)$$

we have

$$p(r) = \frac{\exp \beta - 1}{b - a + (\exp \beta - 1)(r - a)}. \quad (11)$$

The problem is studied within the range $a \leq r \leq b$. In the analysis, the following notations are used:

$$\sigma_r|_{r=a} = \sigma_{r,a}, \quad u|_{r=a} = u_a, \quad (12)$$

$$\sigma_r|_{r=b} = \sigma_{r,b}, \quad u|_{r=b} = u_b. \quad (13)$$

In (12), $\sigma_{r,a}$ and $\sigma_{r,b}$ denote the stress component σ_r at $r = a$ and $r = b$, and u_a and u_b denote the displacement u at $r = a$ and $r = b$, respectively.

For a single-layer cylinder case, there are four possibilities for formulating the boundary problems. They are as follows:

$$\sigma_{r,a} = f_1, \quad \sigma_{r,b} = f_2, \quad (14a)$$

$$\sigma_{r,a} = f_1, \quad u_b = g_2, \quad (14b)$$

$$u_a = g_1, \quad \sigma_{r,b} = f_2, \quad (14c)$$

$$u_a = g_1, \quad u_b = g_2, \quad (14d)$$

where f_1 , f_2 , g_1 , and g_2 are values given beforehand.

2.2. Formulation of the transfer matrix for the case of a single-layer cylinder. Physically, if the two initial values for $\sigma_{r,a}$ and u_a are assumed at $r = a$, we have definite values for $\sigma_{r,b}$ and u_b at $r = b$. This relation can be written in the form

$$\sigma_{r,b} = \mathbf{M}_{11}\sigma_{r,a} + \mathbf{M}_{12}u_a, \quad u_b = \mathbf{M}_{21}\sigma_{r,a} + \mathbf{M}_{22}u_a, \quad (15)$$

or in matrix form

$$\{\sigma_{r,b} \ u_b\}^T = \mathbf{M} \{\sigma_{r,a} \ u_a\}^T. \quad (16)$$

The matrix \mathbf{M} is called the transfer matrix hereafter.

The introduced matrix \mathbf{M} is used not only in the single-layer case but also in the multiply-layered case. In the following analysis, a technique for finding the matrix \mathbf{M} will be introduced. In the first step, two fundamental functions $s_1(r)$ and $s_2(r)$ are introduced:

$$\Lambda(s_1(r)) = 0, \quad s_1|_{r=a} = 1, \quad \left. \frac{ds_1}{dr} \right|_{r=a} = 0 \quad (\text{first fundamental function}), \quad (17)$$

$$\Lambda(s_2(r)) = 0, \quad s_2|_{r=a} = 0, \quad \left. \frac{ds_2}{dr} \right|_{r=a} = 1 \quad (\text{second fundamental function}), \quad (18)$$

where the operator $\Lambda(F(r))$ has been defined by (8).

From the two fundamental solutions and (4), (7), (17), and (18), we have

$$\sigma_r|_{r=a} = \frac{1}{a} \quad \text{and} \quad u|_{r=a} = -\frac{(1+\nu)\nu}{E(a)} \quad \text{for the first fundamental solution } s_1(r), \quad (19)$$

$$\sigma_r|_{r=a} = 0 \quad \text{and} \quad u|_{r=a} = \frac{(1-\nu^2)a}{E(a)} \quad \text{for the first fundamental solution } s_2(r). \quad (20)$$

It is assumed that the studied solution for $F(r)$ is expressed as

$$F(r) = c_1s_1(r) + c_2s_2(r). \quad (21)$$

Thus, from (19), (20) and (21), we have

$$\sigma_{r,a} = \frac{1}{a}c_1, \quad u_a = \frac{(1-\nu^2)a}{E(a)} \left(-\frac{\nu}{(1-\nu)a}c_1 + c_2 \right). \quad (22)$$

Equation (22) may be rewritten as

$$c_1 = a\sigma_{r,a}, \quad c_2 = \frac{\nu}{1-\nu}\sigma_{r,a} + \frac{E(a)}{(1-\nu^2)a}u_a, \quad (23)$$

or in matrix form

$$\{c_1 \ c_2\}^T = \mathbf{Q}\{\sigma_{r,a} \ u_a\}^T, \quad (24)$$

where

$$Q_{11} = a, \quad Q_{12} = 0, \quad Q_{21} = \frac{\nu}{1-\nu}, \quad Q_{22} = \frac{E(a)}{(1-\nu^2)a}. \quad (25)$$

Now we consider the conditions at $r = b$. After numerical integration, from the two fundamental solutions we obtain

$$\sigma_r^{1*}|_{r=b} = \sigma_{r,b}^{1*}, \quad u^{1*}|_{r=b} = u_b^{1*} \quad \text{for the first fundamental solution } s_1(r). \quad (26)$$

$$\sigma_r^{2*}|_{r=b} = \sigma_{r,b}^{2*}, \quad u^{2*}|_{r=b} = u_b^{2*} \quad \text{for the second fundamental solution } s_2(r). \quad (27)$$

The values of $\sigma_{r,b}^{1*}$ and u_b^{1*} can be obtained from (4) and (7) by numerically integrating the expression for $s_1(r)$ and taking $r = b$, and similarly for $\sigma_{r,b}^{2*}$ and u_b^{2*} .

From (21), (26) and (27), we have

$$\sigma_{r,b} = \sigma_{r,b}^{1*}c_1 + \sigma_{r,b}^{2*}c_2, \quad u_b = u_b^{1*}c_1 + u_b^{2*}c_2, \quad (28)$$

or in matrix form

$$\{\sigma_{r,b} \ u_b\}^T = \mathbf{P}\{c_1 \ c_2\}^T, \quad (29)$$

where

$$P_{11} = \sigma_{r,b}^{1*}, \quad P_{12} = \sigma_{r,b}^{2*}, \quad P_{21} = u_b^{1*}, \quad P_{22} = u_b^{2*}. \quad (30)$$

Combining (24) with (29), we have

$$\{\sigma_{r,b} \ u_b\}^T = \mathbf{M} \{\sigma_{r,a} \ u_a\}^T, \quad (31)$$

where the matrix \mathbf{M} is defined by

$$\mathbf{M} = \mathbf{P} \mathbf{Q}. \quad (32)$$

As claimed previously, once the two initial values for $\sigma_{r,a}$ and u_a are assumed at $r = a$, we have definite values for $\sigma_{r,b}$ and u_b at $r = b$. The relation shown by (31) is useful for both the single-layered case and the multiply-layered case.

The evaluation of matrix \mathbf{P} depends on the numerical solution of the ordinary differential equation (8). For example, the two components $P_{11} = \sigma_{r,b}^{1*}$ and $P_{12} = u_b^{1*}$ are results of the initial boundary value problem for function $s_1(r)$ defined by (17). In the numerical integration, the Runge–Kutta method is used [Hildebrand 1974]. The components for matrix \mathbf{Q} have been defined by (25). Finally, the matrix \mathbf{M} can be evaluated from (32) immediately.

Below, we try to solve the boundary value problem

$$\sigma_{r,a} = f_1, \quad \sigma_{r,b} = f_2. \quad (14a)$$

Substituting condition (14a) into (15) or (31) yields

$$f_2 = \mathbf{M}_{11} f_1 + \mathbf{M}_{12} u_a \quad \text{or} \quad u_a = (f_2 - \mathbf{M}_{11} f_1) / \mathbf{M}_{12}. \quad (33)$$

Substituting the given $\sigma_{r,a} = f_1$ value and the value u_a from (33) into (24), two values c_1 and c_2 are obtained. Finally, the function $F(r) = c_1 s_1(r) + c_2 s_2(r)$ shown by (21) is obtained. This means that the whole stress field for the single-layer cylinder is obtainable.

2.3. Numerical solution in single-layer case.

Example 1. In this example, the Young's modulus is $E(r) = E_0 \exp\{\beta(r-a)/(b-a)\}$, defined by (5). The cylinder is subject to an inner pressure q_0 and the boundary conditions take the following form (Figure 1):

$$\sigma_{r,a} = \sigma_r|_{r=a} = -q_0, \quad \sigma_{r,b} = \sigma_r|_{r=b} = 0. \quad (34)$$

Substituting $f_1 = -q_0$ and $f_2 = 0$ into (33), we have $u_a = \mathbf{M}_{11} q_0 / \mathbf{M}_{12}$. As claimed previously, from two values $\sigma_{r,a} (= -q_0)$ and $u_a (= \mathbf{M}_{11} q_0 / \mathbf{M}_{12})$, and two values c_1 and c_2 , the function $F(r) = c_1 s_1(r) + c_2 s_2(r)$ and the whole stress field for the single-layer cylinder are obtainable.

Note that the Young's modulus is expressed by $E(r) = E_0 \exp\{\beta(r-a)/(b-a)\}$, and changes from E_0 at $r = a$ to $E_0 \exp \beta$ at $r = b$. In the solution of the differential equation, $N = 200$ divisions are used in the integration [Hildebrand 1974]. The calculated results for the stresses can be expressed as

$$\sigma_r = f_1(\beta, r) q_0, \quad \sigma_\theta = f_2(\beta, r) q_0, \quad \sigma_e = \sigma_\theta - \sigma_r = f_3(\beta, r) q_0 \quad (f_3 = f_2 - f_1). \quad (35)$$

The calculated results for f_1 , f_2 , and f_3 under the conditions $a/b = 0.5$ and $\beta \in \{-0.5, 0, 0.5, 1, 1.5\}$ are plotted in Figures 2, 3, and 4. Since $E(a) = E_0$ and $E(b) = E_0 \exp \beta$, we have $E(b)/E(a) = 0.6065, 1.0000, 1.6487, 2.7183, \text{ and } 4.4817$ for $\beta = -0.5, 0, 0.5, 1, \text{ and } 1.5$, respectively.

We see from the general theory of strength of materials that the strength of the cylinder mainly depends on the stress component $\sigma_e = \sigma_\theta - \sigma_r$ (or $f_3(\beta, r)$). From Figure 4 we see that the σ_e distribution along the interval $a \leq r \leq b$ varies rapidly in the homogeneous material case. For example, at $\beta = 0$, we have $f_3 = 2.6667, 1.1852,$ and $0.6667,$ for $(r - a)/(b - a) = 0, 0.5,$ and $1.0,$ respectively. In addition, a higher β value can considerably improve the σ_e distribution along the interval $(a \leq r \leq b)$. For example, at $\beta = 1.5,$ we have $f_3 = 1.7283, 1.3428,$ and $1.5045,$ for $(r - a)/(b - a) = 0, 0.5,$ and $1.0,$ respectively. This means that if outer portion of the cylinder is more rigid, the safe condition is better. On the contrary,

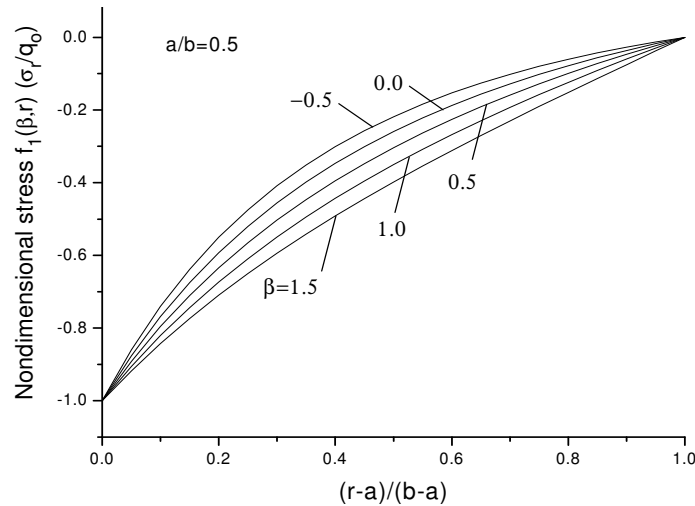


Figure 2. Nondimensional radial stress $f_1(\beta, r)$, for the σ_r component in the cylinder, with $a/b = 0.5,$ inner pressure $q_0,$ and $E(r) = E_0e^{\beta(r-a)/(b-a)}$ (see (35) and Figure 1).

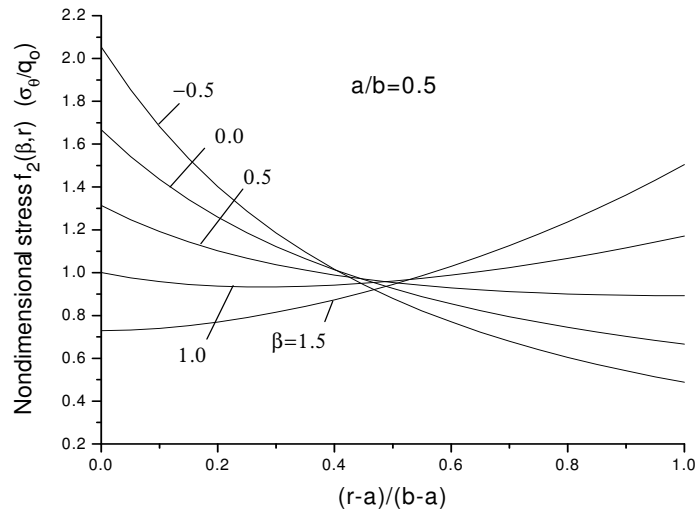


Figure 3. Nondimensional circumferential stress $f_2(\beta, r)$, for the σ_θ component in the cylinder, with $a/b = 0.5,$ inner pressure $q_0,$ and $E(r) = E_0e^{\beta(r-a)/(b-a)}$ (see (35) and Figure 1).

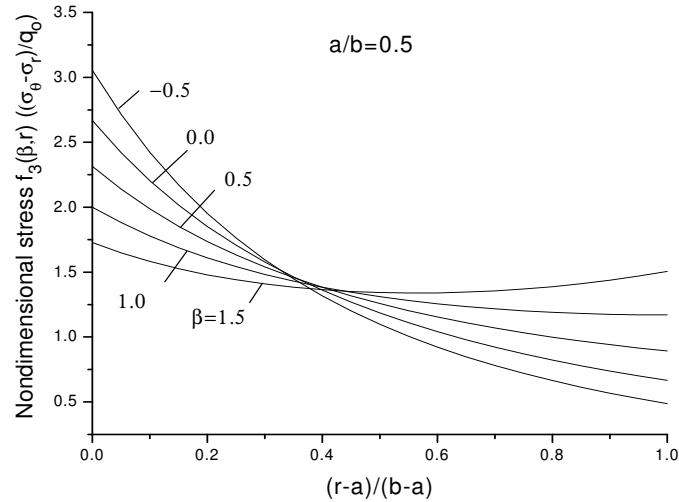


Figure 4. Nondimensional stress $f_3(\beta, r)$, for the $\sigma_e = \sigma_\theta - \sigma_r$ component in the cylinder, with $a/b = 0.5$, inner pressure q_0 , and $E(r) = E_0 e^{\beta(r-a)/(b-a)}$ (see (35) and Figure 1).

if the outer portion of the cylinder is less rigid, the safe condition becomes worse (see the curve for $\beta = -0.5$ in Figure 4). It is found that the plotted results coincide with those obtained previously [Chen and Lin 2008].

Example 2. In this example, the Young's modulus is $E(r) = E_0[1 + (\exp \beta - 1)(r - a)/(r - b)]$, defined by (10). The other computed conditions are the same as in Example 1. The computed stresses are still expressed by (35). The calculated results for f_1 , f_2 , and f_3 , under the conditions $a/b = 0.5$ and $\beta \in \{0.5, 0, 0.5, 1, 1.5\}$ are plotted in Figures 5, 6, and 7.

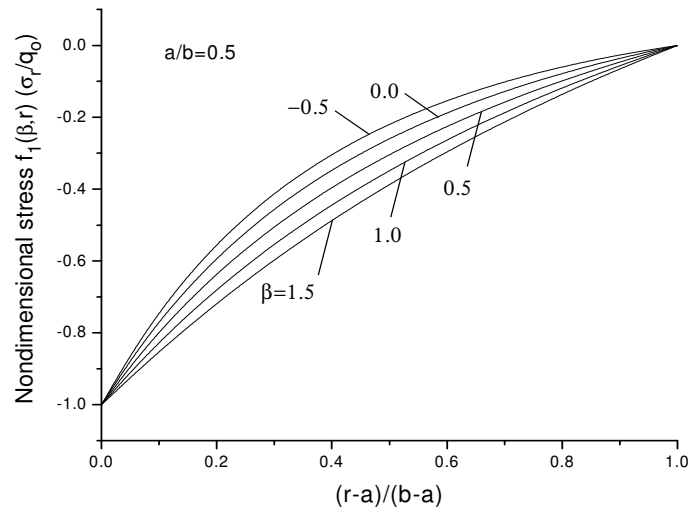


Figure 5. Nondimensional radial stress $f_1(\beta, r)$, for the σ_r component in the cylinder, with $a/b = 0.5$, inner pressure q_0 , and $E(r) = E_0[1 + (e^\beta - 1)(r - a)/(b - a)]$ (see (35) and Figure 1).

In Example 1, for $\beta = 1.5$, we have $f_3 = 1.7283, 1.3428,$ and 1.5045 , for $(r - a)/(b - a) = 0, 0.5,$ and 1.0 , respectively. However, in the present example, using Young’s modulus of linear distribution, we have $f_3 = 1.5398, 1.4289,$ and 1.2626 , for $(r - a)/(b - a) = 0, 0.5,$ and 1.0 , respectively (from Figure 7). The stress distribution in the present case is slightly better than that in Example 1.

In both examples $E(r)|_{r=a} = E_0$ and $E(r)|_{r=b} = E_0 \exp \beta$, Figures 2–4 and Figures 5–7 have similar shapes.

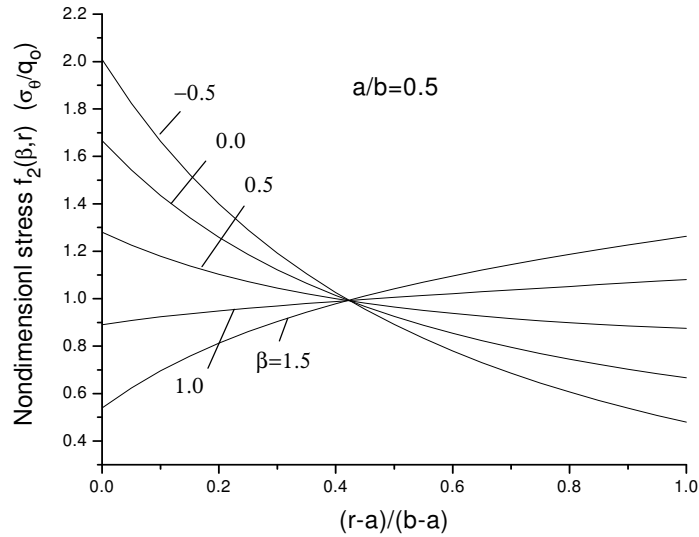


Figure 6. Nondimensional circumferential stress $f_2(\beta, r)$, for the σ_θ component in the cylinder, with $a/b = 0.5$, inner pressure q_0 , and $E(r) = E_0[1 + (e^\beta - 1)(r - a)/(b - a)]$ (see (35) and Figure 1).

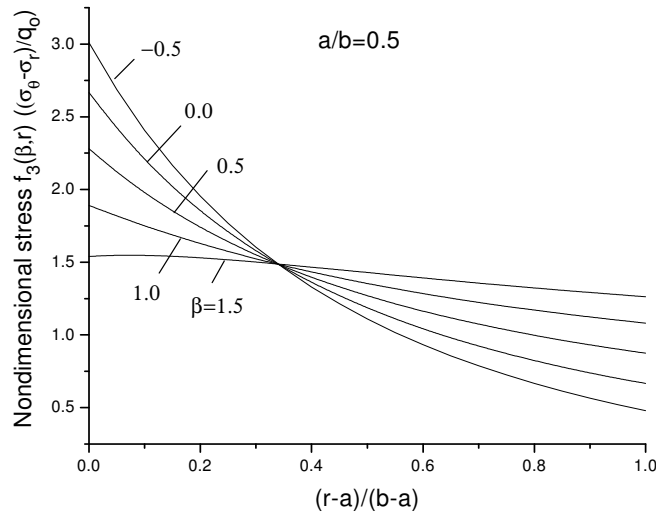


Figure 7. Nondimensional stress $f_3(\beta, r)$, for the $\sigma_e = \sigma_\theta - \sigma_r$ component in the cylinder, with $a/b = 0.5$, inner pressure q_0 , and $E(r) = E_0[1 + (e^\beta - 1)(r - a)/(b - a)]$ (see (35) and Figure 1).

3. Solution for multiply-layered cylinder using the transfer matrix method

Based on the concept of the transfer matrix, a solution for multiply-layered cylinder is introduced below.

3.1. Procedure for the solution of multiply-layered cylinder using the transfer matrix method. The formulation for a cylinder with three layers is introduced below. The cylinder is composed of three layers along the intervals $a_j \leq r \leq b_j$ ($j = 1, 2, 3$) (see Figure 8). In each layer, the Young's elastic modulus is assumed as follows:

$$E^{(j)}(r) = E_0^{(j)} \exp[\beta_j(r - a_j)/c], \quad a_j \leq r \leq b_j \quad (j = 1, 2, 3, \text{ with } c = b - a), \quad (36)$$

where $E_0^{(j)}$ and β_j ($j = 1, 2, 3$) are given beforehand.

In derivation, the boundary values at the initial point for j -th layer ($j = 1, 2, 3$) are denoted by $\sigma_{r,in}^{(j)}, u_{in}^{(j)}$, and at the end point by $\sigma_{r,end}^{(j)}, u_{end}^{(j)}$ ($j = 1, 2, 3$) (see Figure 5). Clearly, the continuation condition between layers can be expressed in the form

$$\sigma_{r,end}^{(j)} = \sigma_{r,in}^{(j+1)}, \quad u_{end}^{(j)} = u_{in}^{(j+1)} \quad (j = 1, 2). \quad (37)$$

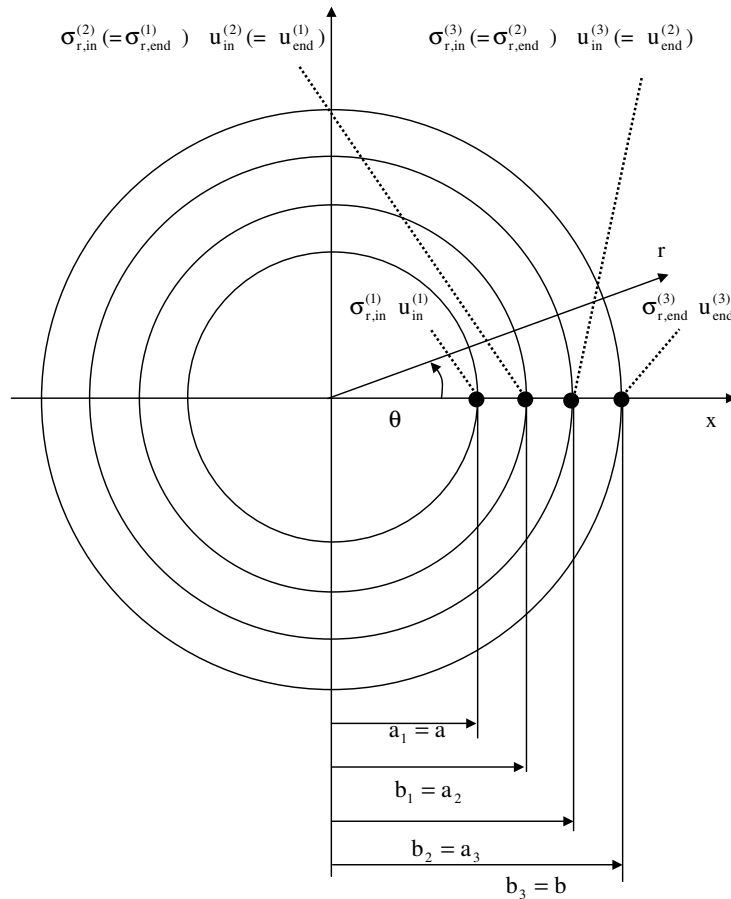


Figure 8. A cylinder with three layers.

In addition, the relevant matrices are denoted by $\mathbf{Q}^{(j)}$, $\mathbf{P}^{(j)}$, and $\mathbf{M}^{(j)}$ ($j = 1, 2, 3$)—see (24) (29), (31), and (32)—and the coefficients before the fundamental solutions by $c_1^{(j)}$ and $c_2^{(j)}$ —(21).

From the analysis in the single-layer case, or from (31), we have

$$\{\sigma_{r,\text{end}}^{(j)} \ u_{\text{end}}^{(j)}\}^T = \mathbf{M}^{(j)} \{\sigma_{r,\text{in}}^{(j)} \ u_{\text{in}}^{(j)}\}^T \quad (j = 1, 2, 3). \tag{38}$$

It is preferable to write (38) in the form

$$\sigma_{r,\text{end}}^{(1)} = \sigma_{r,\text{in}}^{(2)} = M_{11}^{(1)} \sigma_{r,\text{in}}^{(1)} + M_{12}^{(1)} u_{\text{in}}^{(1)}, \quad u_{\text{end}}^{(1)} = u_{\text{in}}^{(2)} = M_{21}^{(1)} \sigma_{r,\text{in}}^{(1)} + M_{22}^{(1)} u_{\text{in}}^{(1)}, \tag{39}$$

$$\sigma_{r,\text{end}}^{(2)} = \sigma_{r,\text{in}}^{(3)} = M_{11}^{(2)} \sigma_{r,\text{in}}^{(2)} + M_{12}^{(2)} u_{\text{in}}^{(2)}, \quad u_{\text{end}}^{(2)} = u_{\text{in}}^{(3)} = M_{21}^{(2)} \sigma_{r,\text{in}}^{(2)} + M_{22}^{(2)} u_{\text{in}}^{(2)}, \tag{40}$$

$$\sigma_{r,\text{end}}^{(3)} = M_{11}^{(3)} \sigma_{r,\text{in}}^{(3)} + M_{12}^{(3)} u_{\text{in}}^{(3)}, \quad u_{\text{end}}^{(3)} = M_{21}^{(3)} \sigma_{r,\text{in}}^{(3)} + M_{22}^{(3)} u_{\text{in}}^{(3)}. \tag{41}$$

From (39)–(41) we see that there are six equations with eight arguments: $\sigma_{r,\text{in}}^{(1)}$, $u_{\text{in}}^{(1)}$, $\sigma_{r,\text{in}}^{(2)}$, $u_{\text{in}}^{(2)}$, $\sigma_{r,\text{in}}^{(3)}$, $u_{\text{in}}^{(3)}$, $\sigma_{r,\text{end}}^{(3)}$, and $u_{\text{end}}^{(3)}$.

When the three-layered cylinder subjected to an inner pressure with intensity q_0 (at $r = a_1 = a$) and the outer boundary is traction free (at $r = b_3 = b$), the following boundary value problem is formulated:

$$\sigma_{r,\text{in}}^{(1)} = -q_0, \quad \sigma_{r,\text{end}}^{(3)} = 0 \quad (\text{or } \sigma_{r,a} = -q_0, \sigma_{r,b} = 0). \tag{42}$$

Substituting this condition into (39), we will obtain a solution for six unknowns $u_{\text{in}}^{(1)}$, $\sigma_{r,\text{in}}^{(2)}$, $u_{\text{in}}^{(2)}$, $\sigma_{r,\text{in}}^{(3)}$, $u_{\text{in}}^{(3)}$, and $u_{\text{end}}^{(3)}$ from the six algebraic equations (39)–(41). In addition, from (24), we have

$$\{c_1^{(j)} \ c_2^{(j)}\}^T = \mathbf{Q}^{(j)} \{\sigma_{r,a}^{(j)} \ u_a^{(j)}\}^T \quad (j = 1, 2, 3). \tag{43}$$

Finally, the undetermined coefficients $c_1^{(j)}$ and $c_2^{(j)}$ ($j = 1, 2, 3$) before the fundamental solutions are obtained. This means that the final solution is obtained.

Clearly, if the boundary condition is different from the one in (42), the problem can be solved in a similar manner.

3.2. Numerical example for three-layered cylinder.

Example 3. In Example 1, the case of $\beta = 1.5$ can provide a better distribution for the stress component $\sigma_e = \sigma_\theta - \sigma_r$. In the present example, a modification for this case is carried out. For the case of three layers, the Young’s elastic modulus is assumed as follows (see Figure 8):

$$E^{(1)}(r) = E_0 \exp \frac{\beta(1-\alpha)(r-a_1)}{c} \quad (a_1 \leq r \leq b_1, \text{ with } c = b-a), \tag{44a}$$

$$E^{(2)}(r) = E_0^{(2)} \exp \frac{\beta(r-a_2)}{c} \quad (a_2 \leq r \leq b_2), \tag{44b}$$

$$E^{(3)}(r) = E_0^{(3)} \exp \frac{\beta(1+\alpha)(r-a_3)}{c} \quad (a_3 \leq r \leq b_3), \tag{44c}$$

where $a_1 = a$, $a_2 = b_1 = (2a + b)/3$, $a_3 = b_2 = (a + 2b)/3$, and $b_3 = b$. In (44), the factor α represents a modification to the case shown by (5).

From the continuation condition for $E^{(j)}(r)$ ($j = 1, 2, 3$), at $r = a_2$ and $r = a_3$, we find

$$E_0^{(2)} = E_0 \exp \frac{\beta(1-\alpha)}{3}, \quad E_0^{(3)} = E_0 \exp \frac{\beta(2-\alpha)}{3}. \tag{45}$$

When the three-layered cylinder is subjected to an inner pressure with intensity q_0 (at $r = a_1 = a$) and the outer boundary is traction free (at $r = b_3 = b$), the following boundary value problem is formulated:

$$\sigma_{r,\text{in}}^{(1)} = -q_0, \quad \sigma_{r,\text{end}}^{(3)} = 0 \quad (\text{or } \sigma_{r,a} = -q_0 \text{ at } r = a, \sigma_{r,b} = 0 \text{ at } r = b). \quad (46)$$

The procedure for the solution has been suggested in the last section. In the computation, we choose $a/b = 0.5$, $\beta = 1.5$, and $\alpha \in \{-0.5, -0.25, 0, 0.25, 0.5\}$. The assumed Young's modulus is denoted by

$$E(r) = h(\beta, \alpha, r)E_0. \quad (47)$$

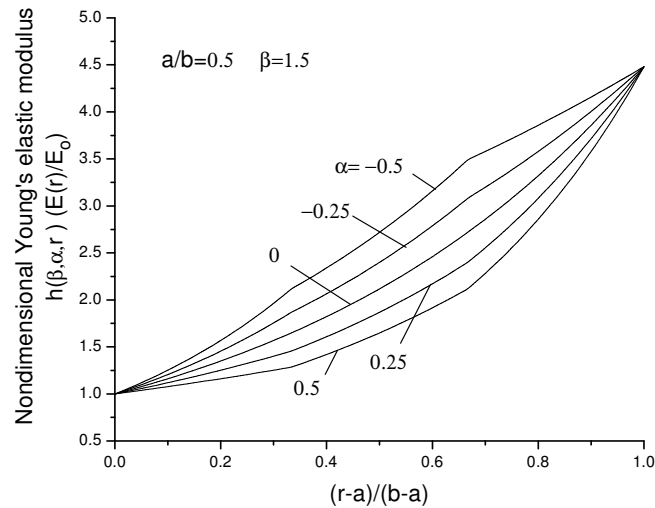


Figure 9. Young's elastic modulus $h(\beta, \alpha, r)$ ($E(r)/E_0$) (see (44), (45), (47), and Figure 8).

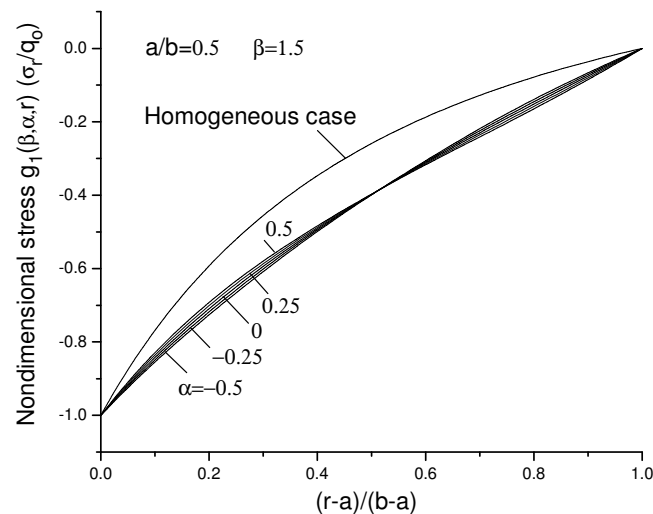


Figure 10. Nondimensional radial stress $g_1(\beta, \alpha, r)$, for the σ_r component in a three-layer cylinder, with $a/b = 0.5$ and $\sigma_{r,a} = -q_0$, $\sigma_{r,b} = 0$ (see (48) and Figure 8).

In addition, the computed stresses are expressed by

$$\sigma_r = g_1(\beta, \alpha, r)q_0, \quad \sigma_\theta = g_2(\beta, \alpha, r)q_0, \quad \sigma_e = \sigma_\theta - \sigma_r = g_3(\beta, \alpha, r)q_0 \quad (g_3 = g_2 - g_1). \quad (48)$$

The function $h(\beta, \alpha, r)$ and the computed $g_1(\beta, \alpha, r)$, $g_2(\beta, \alpha, r)$, and $g_3(\beta, \alpha, r)$ are plotted in Figures 9–12. For the homogeneous case of the Young’s modulus or $\beta = 0$, the relevant results are also plotted in those figures.

It is seen from Figure 12 that the condition of $\beta = 1.5$ and $\alpha = -0.5$ can provide a better distribution for the σ_e component. In fact, in the homogeneous case ($\beta = 0$), we have $\sigma_e = 0.6667$ at $r = a$, and

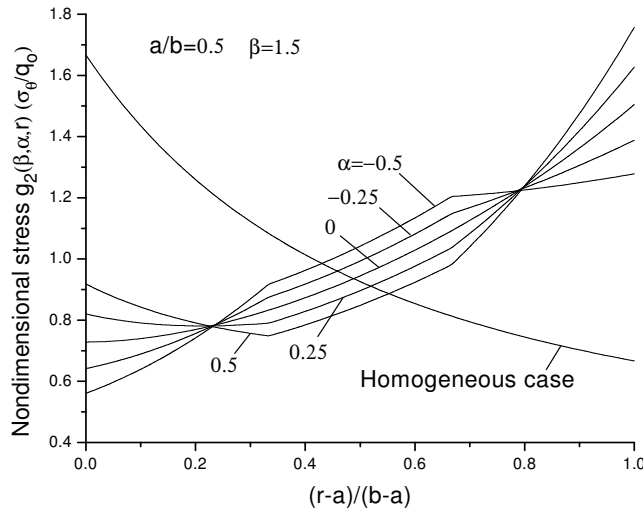


Figure 11. Nondimensional circumferential stress $g_2(\beta, \alpha, r)$, for the σ_θ component in a three-layer cylinder, with $a/b = 0.5$ and $\sigma_{r,a} = -q_0$, $\sigma_{r,b} = 0$ (see (48) and Figure 8).

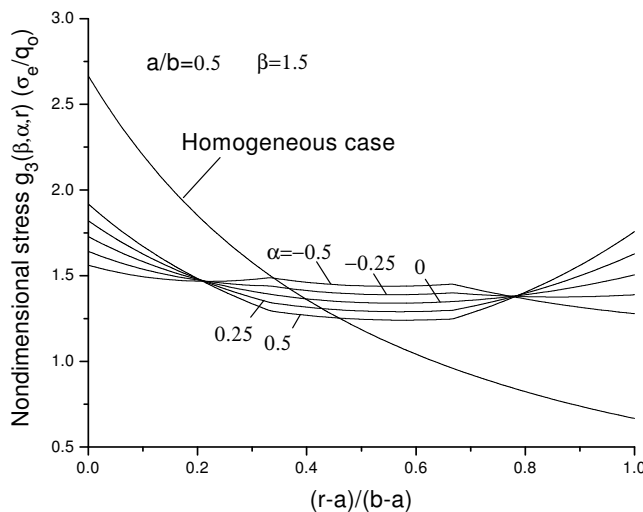


Figure 12. Nondimensional stress $g_3(\beta, \alpha, r)$, for the $\sigma_e = \sigma_\theta - \sigma_r$ component in a cylinder of three layers, with $a/b = 0.5$ and $\sigma_{r,a} = -q_0$, $\sigma_{r,b} = 0$ (see (48) and Figure 8).

$\frac{r-a}{b-a}$	N	$\alpha = -0.5$	$\alpha = -0.25$	$\alpha = 0$	$\alpha = 0.25$	$\alpha = 0.5$
1/6	40	0.7050683358	0.7319400382	0.7577991468	0.7825211369	0.8059881607
1/6	120	0.7050683357	0.7319400381	0.7577991467	0.7825211368	0.8059881604
1/6	200	0.7050683357	0.7319400381	0.7577991467	0.7825211368	0.8059881604
1/2	40	1.0416074339	0.9931088747	0.9446411237	0.8963340949	0.8483207310
1/2	120	1.0416074337	0.9931088746	0.9446411236	0.8963340948	0.8483207308
1/2	200	1.0416074337	0.9931088746	0.9446411236	0.8963340948	0.8483207308
5/6	40	1.2327192411	1.2559360854	1.2771271334	1.2961108296	1.3127162028
5/6	120	1.2327192410	1.2559360853	1.2771271333	1.2961108295	1.3127162025
5/6	200	1.2327192410	1.2559360853	1.2771271333	1.2961108295	1.3127162025

Table 1. Comparison results for nondimensional radial stress $g_2(\beta, \alpha, r)$, for the σ_θ component in a three-layer cylinder, with $a/b = 0.5$, $\beta = 1.5$, and $\sigma_{r,a} = -q_0$, $\sigma_{r,b} = 0$, and various numbers N of intervals used in the integration. See (48) and Figure 8.

$\sigma_e = 2.6667$ at $r = b$. Thus, the ratio $\sigma_e|_{r=b}/\sigma_e|_{r=a} = 0.25$ is achieved. That is to say, the outer boundary has too high a safety factor when σ_e at the inner boundary point reaches its limit value. However, under condition $\beta = 1.5$ and $\alpha = -0.5$, we have $\sigma_e = 1.5609$ at $r = a$, and $\sigma_e = 1.2785$ at $r = b$. In this case, the relative ratio is $\sigma_e|_{r=b}/\sigma_e|_{r=a} = 0.8087$.

To gauge the accuracy of the computations, some results for $g_2(\beta, \alpha, r)$ ($\sigma_e = q_0$) were calculated using $N = 40, 120$, and 200 divisions in the integration. They are listed in Table 1, where we see that even 40 divisions suffice to give an accuracy of nine decimals. The choice $N = 200$ was far beyond the necessary divisions for providing accurate results.

Example 4. In this example, all parameters, $E_0, \beta, \alpha, a_1 = a, a_2 = b_1 = (2a + b)/3, a_3 = b_2 = (a + 2b)/3$, and $b_3 = b$, are the same as those used in Example 1. However, the following boundary condition is

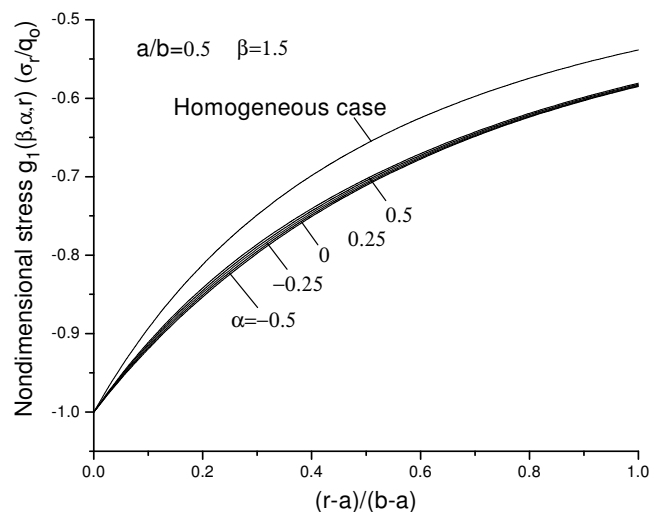


Figure 13. Nondimensional radial stress $g_1(\beta, \alpha, r)$, for the σ_r component in a three-layer cylinder, with $a/b = 0.5$ and $\sigma_{r,a} = -q_0, u_b = 0$ (see (48) and Figure 8).

assumed:

$$\sigma_{r,in}^{(1)} = -q_0, \quad u_{end}^{(3)} = 0 \quad (\text{or } \sigma_{r,a} = -q_0 \text{ at } r = a, \quad u_b = 0 \text{ at } r = b). \quad (49)$$

In this case, substituting $\sigma_{r,in}^{(1)} = -q_0, u_{end}^{(3)} = 0$, into (39), we have a solution for $u_{in}^{(1)}, \sigma_{r,in}^{(2)}, u_{in}^{(2)}, \sigma_{r,in}^{(3)}, u_{in}^{(3)}$, and $\sigma_{r,end}^{(3)}$. The further steps are the same as in Example 3.

In computation, we choose $a/b = 0.5, \beta = 1.5, \alpha = -0.50, -0.25, 0, 0.25$ and 0.5 . The assumed Young's modulus $E(r) = h(\beta, \alpha, r)E_0$ is same as shown by (47). The computed stresses $\sigma_r = g_1(\beta, \alpha, r)q_0, \sigma_\theta = g_2(\beta, \alpha, r)q_0, \sigma_e = \sigma_\theta - \sigma_r = g_3(\beta, \alpha, r)q_0$ ($g_3 = g_2 - g_1$), are still expressed by (48).

The function $h(\beta, \alpha, r)$ is the same as plotted in Figure 9. The computed $g_1(\beta, \alpha, r), g_2(\beta, \alpha, r)$, and $g_3(\beta, \alpha, r)$ are plotted in Figures 13–15.

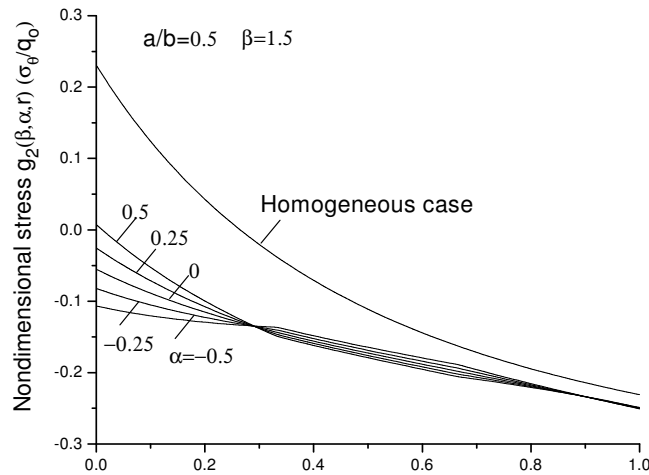


Figure 14. Nondimensional circumferential stress $g_2(\beta, \alpha, r)$, for the σ_θ component in a three-layer cylinder, with $a/b = 0.5$ and $\sigma_{r,a} = -q_0, u_b = 0$ (see (48) and Figure 5).

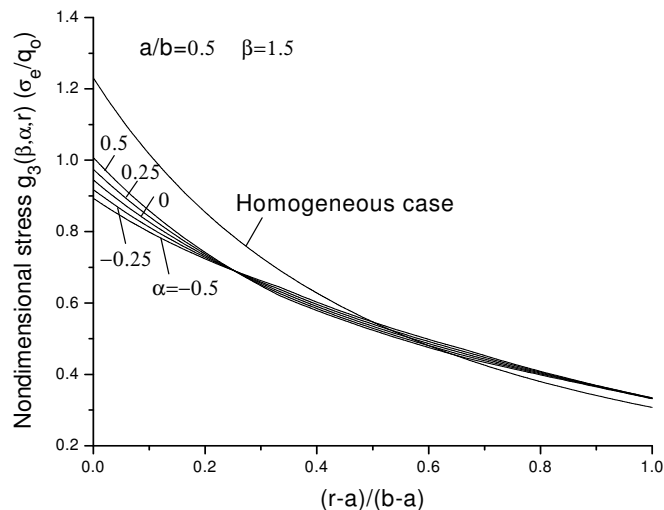


Figure 15. Nondimensional stress $g_3(\beta, \alpha, r)$, for the $\sigma_e = \sigma_\theta - \sigma_r$ component in a cylinder of three layers, with $a/b = 0.5$ and $u_b = 0, \sigma_{r,b} = 0$ (see (48) and Figure 5).

It is seen from Figure 15 that the condition $\beta = 1.5$ and $\alpha = -0.5$ can provide a better distribution for the σ_e component. In fact, in the homogeneous case (or $\beta = 0$), we have $\sigma_e = 1.2308$ at $r = a$, and $\sigma_e = 0.3077$ at $r = b$. Thus, the ratio $\sigma_e|_{r=b}/\sigma_e|_{r=a} = 0.25$ is achieved. That is to say, the outer boundary has too much safety factor when σ_e at the inner boundary point reaches its limit value. However, under the condition $\beta = 1.5$ and $\alpha = -0.5$, we have $\sigma_e = 0.8934$ at $r = a$, and $\sigma_e = 0.3343$ at $r = b$. In this case, the relative ratio is $\sigma_e|_{r=b}/\sigma_e|_{r=a} = 0.3742$.

However, in Example 4, the improvement for the σ_e component is not as much as in Example 3. For example, we have $\sigma_e|_{r=b}/\sigma_e|_{r=a} = 0.8087$ and 0.3742 in Examples 3 and 4, respectively, which can be seen from Figures 12 and 15.

4. Conclusion

The transfer matrix method provides an effective way to solve the problem of a multiply-layered cylinder of functionally graded materials (FGMs). In fact, the transfer matrix for the j -th layer links the radial stress and displacement at the initial point to those at the end point of the layer. Those matrices for all layers can be computed and prepared beforehand, and are obtained from two fundamental solutions. After linking all matrices and considering the continuation condition between layers and the boundary conditions, the original problem is solved. In the formulation, the Young's modulus can be arbitrary for the individual layer. In addition, the solution of the mixed boundary value problem is easy to evaluate.

The merit of the suggested method can be expressed alternatively. In fact, the differential operator defined in the left hand of (8) has the following property:

$$\Lambda(cs(r)) = c\Lambda(s(r)) \quad (c \text{ is a constant}). \quad (50)$$

Therefore, if $s_1(r)$ and $s_2(r)$ are two solutions of the ordinary differential equation

$$\Lambda(s(r)) = 0, \quad (51)$$

the function $s(r) = c_1s_1(r) + c_2s_2(r)$ must be a solution of (51). Clearly, the suggested solutions $s_1(r)$ and $s_2(r)$ are the solutions from two particular initial conditions. Once the two constants c_1 and c_2 are appropriately assumed, the boundary condition at the end point ($r = b$) will be satisfied. That is to say, the boundary value problem of the ordinary differential equation is changed into the initial boundary value problem.

It is found from the computed results that the influence of the inhomogeneity from FGMs on the stress distribution is significant. From the theory of strength of materials, the stress component $\sigma_e = \sigma_\theta - \sigma_r$ is an appropriate value to predict the component's safety. From Figure 4, we see that a higher value of β , for example $\beta = 1.5$ can provide a better distribution for σ_e . Alternatively speaking, if the outer layer ($r = b$) is more rigid, the safe condition of cylinder is better.

References

- [Batra and Iaccarino 2008] R. C. Batra and G. L. Iaccarino, "Exact solutions for radial deformations of a functionally graded isotropic and incompressible second-order elastic cylinder", *Int. J. Non-Linear Mech.* **43**:5 (2008), 383–398.
- [Chen and Lin 2008] Y. Z. Chen and X. Y. Lin, "Elastic analysis for thick cylinders and spherical pressure vessels made of functionally graded materials", *Comput. Mater. Sci.* **44**:2 (2008), 581–587.

- [Dryden and Jayaraman 2006] J. Dryden and K. Jayaraman, "Effect of inhomogeneity on the stress in pipes", *J. Elasticity* **83**:2 (2006), 179–189.
- [Erdogan and Wu 1997] F. Erdogan and B. H. Wu, "The surface crack problem for a plate with functionally graded properties", *J. Appl. Mech. (ASME)* **64**:3 (1997), 449–456.
- [Eslami et al. 2005] M. R. Eslami, M. H. Babaei, and R. Poutangari, "Thermal and mechanical stresses in a functionally graded thick sphere", *Int. J. Pres. Ves. Pip.* **82**:7 (2005), 522–527.
- [Fotuhi and Fariborz 2006] A. R. Fotuhi and S. J. Fariborz, "Anti-plane analysis of a functionally graded strip with multiple cracks", *Int. J. Solids Struct.* **43**:5 (2006), 1239–1252.
- [Hildebrand 1974] F. B. Hildebrand, *Introduction to numerical analysis*, 2nd ed., McGraw-Hill, New York, 1974.
- [Horgan and Chan 1999a] C. O. Horgan and A. M. Chan, "The pressurized hollow cylinder or disk problem for functionally graded isotropic linearly elastic materials", *J. Elasticity* **55**:1 (1999), 43–59.
- [Horgan and Chan 1999b] C. O. Horgan and A. M. Chan, "The stress response of functionally graded isotropic linearly elastic rotating disks", *J. Elasticity* **55**:3 (1999), 219–230.
- [Jain et al. 2004] N. Jain, C. E. Rousseau, and A. Shukla, "Crack-tip stress fields in functionally graded materials with linearly varying properties", *Theor. Appl. Fract. Mech.* **42**:2 (2004), 155–170.
- [Li and Peng 2009] X.-F. Li and X.-L. Peng, "A pressurized functionally graded hollow cylinder with arbitrarily varying material properties", *J. Elasticity* **96**:1 (2009), 81–95.
- [Muskhelishvili 1963] N. I. Muskhelishvili, *Some basic problems of the mathematical theory of elasticity. Fundamental equations, plane theory of elasticity, torsion and bending*, P. Noordhoff, Groningen, 1963.
- [Shao 2005] Z. S. Shao, "Mechanical and thermal stresses of a functionally graded circular hollow cylinder with finite length", *Int. J. Pres. Ves. Pip.* **82**:3 (2005), 155–163.
- [Shi et al. 2007] Z. Shi, T. Zhang, and H. Xiang, "Exact solutions of heterogeneous elastic hollow cylinders", *Compos. Struct.* **79**:1 (2007), 140–147.
- [Theotokoglou and Stampouloglou 2008] E. E. Theotokoglou and I. H. Stampouloglou, "The radially nonhomogeneous elastic axisymmetric problem", *Int. J. Solids Struct.* **45**:25-26 (2008), 6535–6552.
- [Timoshenko and Goodier 1970] S. P. Timoshenko and J. N. Goodier, *Theory of elasticity*, McGraw-Hill, New York, 1970.
- [Tutuncu 2007] N. Tutuncu, "Stresses in thick-walled FGM cylinders with exponentially-varying properties", *Eng. Struct.* **29**:9 (2007), 2032–2035.
- [Tutuncu and Temel 2009] N. Tutuncu and B. Temel, "A novel approach to stress analysis of pressurized FGM cylinders, disks and spheres", *Compos. Struct.* **91**:3 (2009), 385–390.
- [You et al. 2005] L. H. You, J. J. Zhang, and X. Y. You, "Elastic analysis of internally pressurized thick-walled spherical pressure vessels of functionally graded materials", *Int. J. Pres. Ves. Pip.* **82**:5 (2005), 347–354.
- [Zhang and Hasebe 1999] X. Zhang and N. Hasebe, "Elasticity solution for a radially nonhomogeneous hollow circular cylinder", *J. Appl. Mech. (ASME)* **66**:3 (1999), 598–606.

Received 4 Mar 2010. Revised 11 May 2010. Accepted 12 May 2010.

Y. Z. CHEN: chens@ujs.edu.cn

Division of Engineering Mechanics, Jiangsu University, Xue Fu Road 301, Jiangsu, 212013, China

JOURNAL OF MECHANICS OF MATERIALS AND STRUCTURES

jomms.org

Founded by Charles R. Steele and Marie-Louise Steele

EDITORS

CHARLES R. STEELE Stanford University, USA
DAVIDE BIGONI University of Trento, Italy
IWONA JASIUK University of Illinois at Urbana-Champaign, USA
YASUhide SHINDO Tohoku University, Japan

EDITORIAL BOARD

H. D. BUI École Polytechnique, France
J. P. CARTER University of Sydney, Australia
R. M. CHRISTENSEN Stanford University, USA
G. M. L. GLADWELL University of Waterloo, Canada
D. H. HODGES Georgia Institute of Technology, USA
J. HUTCHINSON Harvard University, USA
C. HWU National Cheng Kung University, Taiwan
B. L. KARIHALOO University of Wales, UK
Y. Y. KIM Seoul National University, Republic of Korea
Z. MROZ Academy of Science, Poland
D. PAMPLONA Universidade Católica do Rio de Janeiro, Brazil
M. B. RUBIN Technion, Haifa, Israel
A. N. SHUPIKOV Ukrainian Academy of Sciences, Ukraine
T. TARNAI University Budapest, Hungary
F. Y. M. WAN University of California, Irvine, USA
P. WRIGGERS Universität Hannover, Germany
W. YANG Tsinghua University, China
F. ZIEGLER Technische Universität Wien, Austria

PRODUCTION contact@msp.org

SILVIO LEVY Scientific Editor

Cover design: Alex Scorpan

Cover photo: Wikimedia Commons

See <http://jomms.org> for submission guidelines.

JoMMS (ISSN 1559-3959) is published in 10 issues a year. The subscription price for 2011 is US \$520/year for the electronic version, and \$690/year (+\$60 shipping outside the US) for print and electronic. Subscriptions, requests for back issues, and changes of address should be sent to Mathematical Sciences Publishers, Department of Mathematics, University of California, Berkeley, CA 94720–3840.

JoMMS peer-review and production is managed by EditFLOW™ from Mathematical Sciences Publishers.

PUBLISHED BY
 **mathematical sciences publishers**
<http://msp.org/>

A NON-PROFIT CORPORATION

Typeset in L^AT_EX

Copyright ©2011 by Mathematical Sciences Publishers

Journal of Mechanics of Materials and Structures

Volume 6, No. 5

May 2011

- Study of multiply-layered cylinders made of functionally graded materials using the transfer matrix method** **Y. Z. CHEN 641**
- Computational shell mechanics by helicoidal modeling, I: Theory**
TEODORO MERLINI and MARCO MORANDINI 659
- Computational shell mechanics by helicoidal modeling, II: Shell element**
TEODORO MERLINI and MARCO MORANDINI 693
- Effective property estimates for heterogeneous materials with cocontinuous phases**
PATRICK FRANCIOSI, RENALD BRENNER and ABDERRAHIM EL OMRI 729
- Consistent loading for thin plates**
ISAAC HARARI, IGOR SOKOLOV and SLAVA KRYLOV 765



1559-3959(2011)6:5;1-B